Structure Analysis of Metal(I) Halides Mixed Crystal by ^{63}Cu MAS NMR and X-Ray Diffraction Methods. I. $Cu_xAg_{1-x}I$ Crystal

Kazunaka ENDO* and Teruaki FUJITO†
Tsukuba Research Laboratory, Mitsubishi Paper Mills, Ltd., 46 Wadai, Tsukuba-City, Ibaraki 300-42
†NM Group, Analytical Instrument Engineering Department, JEOL Ltd., Akishima, Tokyo 196
(Received December 21, 1989)

^{63}Cu MAS NMR and X-ray diffraction methods have been used to perform a structure analysis of mixed crystals, $Cu_xAg_{1-x}I$. The mixed crystals were prepared and analyzed as a complete solid-solution and a core-shell type of crystal by the X-ray diffraction method. ^{63}Cu signals in the complete solid-solution shifted with broadening to a high field around 14—33 ppm relative to solid CuI, as the silver/copper ratio increased. The line width of the signal was 2-to 2.5-times as broad as that for solid CuI. On the othe hand, the signal in a core-shell type of crystal did not shift much and the line width was much the same as that for CuI. The shifts and broad line widths in the complete solid-solution can be explained by considering components which involve the second-order quadrupolar coupling tensors. The quadrupolar coupling tensors are seen to be caused by changing from T_d of $-(CuI_4)-$ spcies to its C_{3v} and C_{2v} symmetries due to replacing Cu with Ag in the crystal.

We are interested in copper(I) and silver halides as photosensitive and semiconductive materials and catalysts in organic reactions. We think that it is a useful step for discovering new materials to produce mixed crystals. It is well-known that mixed crystals are produced so as to change the property of the material as a single-component crystal. For example, in photographic materials,[1] in order to increase the sensitivity and image quality, we first synthesized solid-solution silver bromochloride, then converted silver iodochloride and the core-shell type of silver iodobromide emulsions.

As necessary conditions to form mixed crystals, we know that the crystal lattices resemble each other and that the atomic radii in the crystals are slightly different. CuI and AgI crystals in this study were of cubic zincblende structure. Those crystals satisfy such conditions. We thus produced two types of mixed crystals: a complete solid-solution by the melt-annealing method and a core-shell type of crystal by a conversion process in an aqueous suspension by using the solubility difference between CuI and AgI. Here, we demonstrate that the ^{63}Cu MAS(magic angle spinning) NMR method can be used to determine the local crystal structre of mixed $Cu_xAg_{1-x}I$.

MAS is a powerful technique routinely used in solid state NMR.[2,3] For spin $I>1/2$ nuclei, MAS can only diminish and modify the second-order quadrupolar line broadening in the NMR spectra;[4-6] it is not possible to average it to zero. This is because of their large quadrupolar coupling, e^2qQ/h, to the electric field gradient, which extends to more than a few MHz in some samples. However, the $Cu_xAg_{1-x}I$ crystal in this study has a cubic zincblende structure; we believe that the $-(CuI_4)-$ species in the unit lattice is very close to tetrahedral symmetry. Thus, a remarkable line-narrowing by MAS can be observed in this crystal.

A structure analysis of the two types of crystals has been performed by X-ray diffraction. Furthermore, by MAS NMR, we obtained ^{63}Cu signals shifted with broadening relative to those of solid CuI, as the silver/copper ratio increased. On the other hand, the signal in a core-shell type of crystal showed almost no shift and the line width was much the same as that of CuI. The results obtained by MAS NMR will be analyzed by considering the local atomic structure of the unit cell due to replacing a Cu atom with a Ag one in zincblende $Cu_xAg_{1-x}I$. The signals in a complete solid-solution can be interpreted by considering the components which involve second-order quadrupolar coupling tensors.[5] The quadrupolar coupling tensors seem to be caused by changing from T_d to C_{3v} and C_{2v} symmetries of $-(CuI_4)-$ species, due to replacing a Cu atom with a Ag one in the crystal.

Experimental

Materials. A complete solid-solution of mixed $Cu_xAg_{1-x}I$ crystal was prepared at 600 °C by the melt-annealing method from CuI and AgI. On the other hand, we prepared a core-shell type of mixed $Cu_xAg_{1-x}I$ crystal by using the solubility difference between CuI and AgI. The crystal was synthesized by a conversion process in a CuI suspension with a gradual addition of an $AgNO_3$ solution by stirring at 60 °C for 30 minutes. After several decantations, the sample was dehydrated in a drying machine at 60 °C for 6 hours. The CuI used here was commercially available.

NMR and X-Ray Diffraction Instruments. The ^{63}Cu MAS NMR spectra of mixed crysrtals were measured at a ^{63}Cu frequency of 71.47 MHz using a JEOL GX-270 spectrometer equipped with an SH 270 unit; 40 transients were accumulated using a 5.5 μs (90°) pulse. All of the spectra were obtained under the conditions of proton gated decoupling and magic angle spinning; 8 K data points were collected over a band width of 50 KHz. Kel-F rotors were used at a spinning speed of about 4.0 MHz. All measurements carried out at room temperature and solid CuCl

(125 Hz for the half width) was used as an external reference. The ratio Cu/Ag for mixed crystals was estimated by using the X-ray fluorescence method. X-Ray diffraction measurements were performed using a Rigaku RAD C.

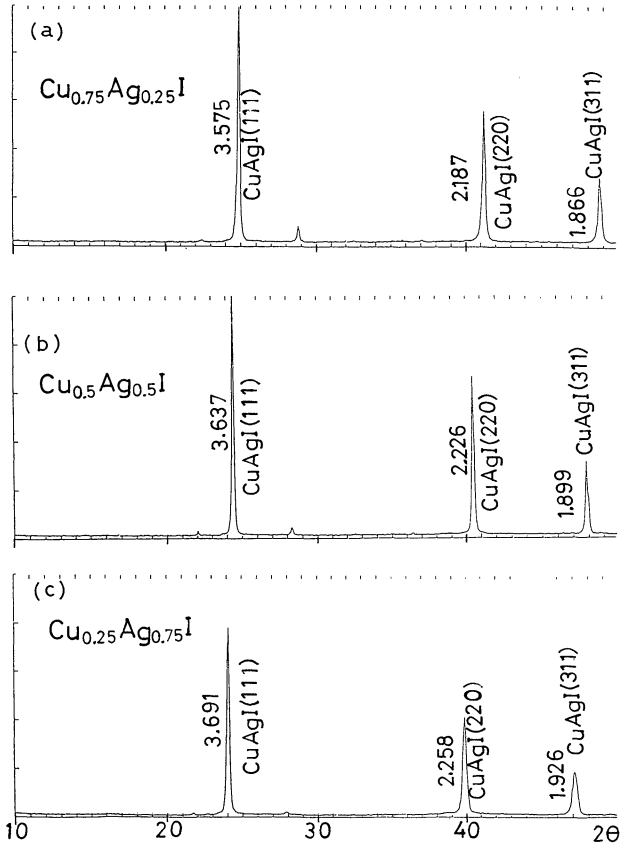

Fig. 1. X-Ray diffraction profiles of complete solid-solution $Cu_xAg_{1-x}I$ crystal versus AgI/CuI ratios.

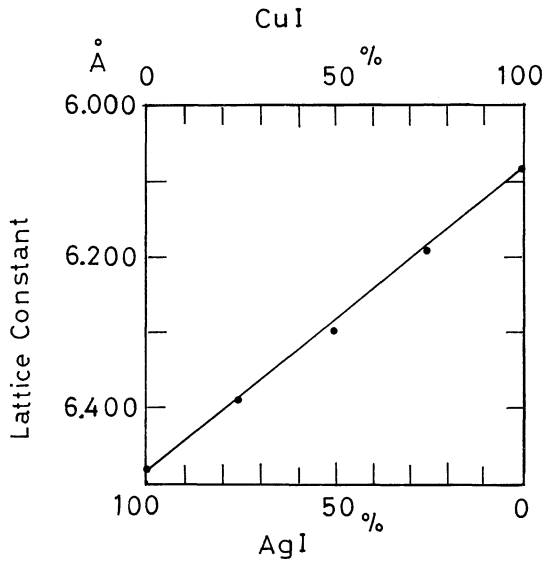

Fig. 2. The unit cell dimension of complete solid-solution $Cu_xAg_{1-x}I$ crystal versus CuI/AgI ratios: The solid line is Vegard law.

Results

(a) Solid-Solution of $Cu_xAg_{1-x}I$ Crystal. Figure 1, (a), (b), and (c) show X-ray diffraction profiles of the $Cu_xAg_{1-x}I$ crystal. This indicates that the mixed crystal has a cubic zincblende structure. These diffraction patterns show that the lattice parameter changes linearly with the Cu and Ag concentration without any change in the crystal structure. The unit cell dimension in Fig. 2 follows well the Vegard[7] law. Thus, the $Cu_xAg_{1-x}I$ crystal is a complete solid solution.

As shown in (a), (b), and (c) in Fig. 3, ^{63}Cu MAS NMR signals of the mixed crystal shifted with broadening to a high field relative to solid CuI (−1.5 ppm and 256 Hz for the chemical shift and half-width). The shift differences and half widths for Ag/Cu ratios of 1/3, 1/1, and 3/1, respectively, are shown in Table 1. The reason can be explained by considering the components which involve the second-order quadrupolar coupling tensors. The coupling tensors are caused by changing from the tetrahedral symmetry of $-(CuI_4)-$ species due to replacing Cu with Ag in the unit lattice.

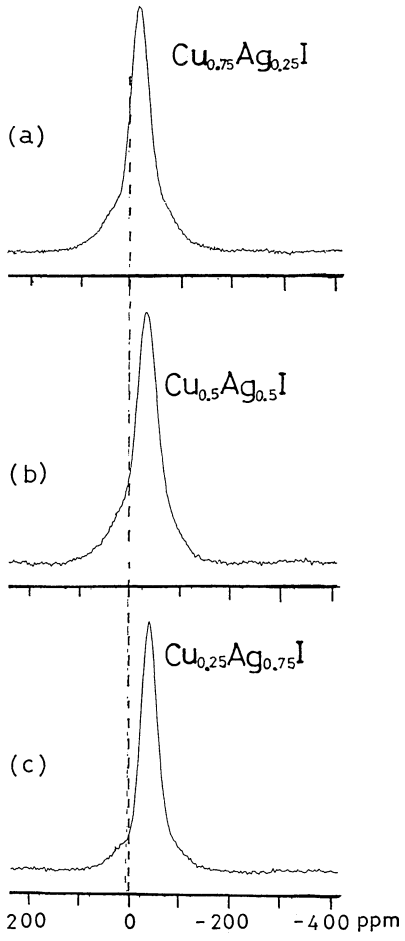

Fig. 3. ^{63}Cu MAS NMR spectra of complete solid-solution $Cu_xAg_{1-x}I$ crystal versus CuI/AgI ratios.

Table 1. ^{63}Cu Chemical Shifts, Half-Linewidths, Quadrupole Coupling Constants and CuI_4 Symmetry of Complete Solid Solution $Cu_xAg_{1-x}I$ for AgI/CuI Ratios

	AgI/CuI ratio		
	1/3	1/1	3/1
Chemical Shifts (ppm)[a)]	14.1	26.9	32.9
Half-Linewidths (Hz)	1608	1805	1427
e^2qQ(MHz)	0.27	0.37	0.41
CuI_4 Symmetry[b)]	C_{3v}	C_{2v}	C_{3v}^+

a) Chemical shifts was refered from CuI. b) Symmetries of C_{3v}, C_{2v}, and C_{3v}^+ correspond to $-Cu_3AgI_4-$, $-Cu_2Ag_2I_4-$ and $-CuAg_3I_4-$ unit cells, respectively.

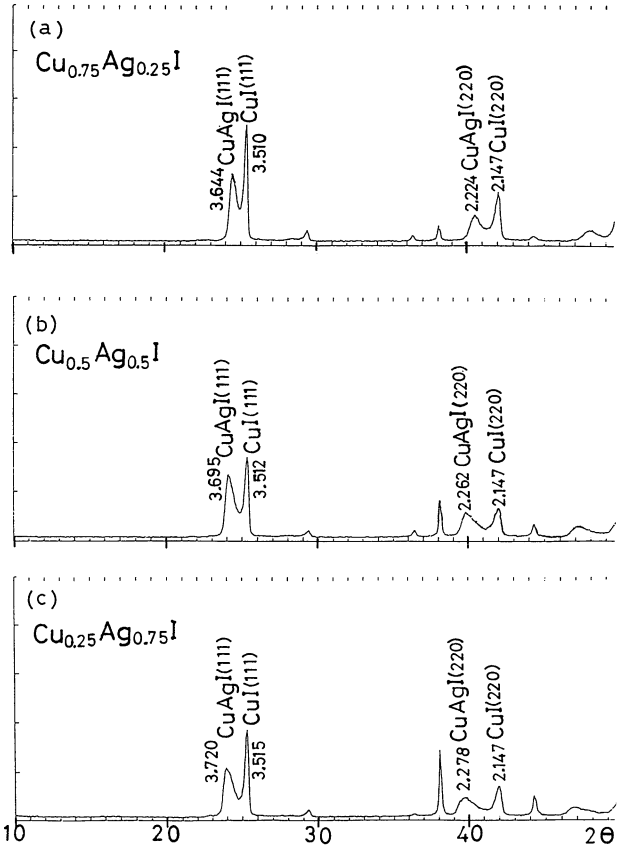

Fig. 4. X-Ray diffraction curves of core-shell types of $Cu_xAg_{1-x}I$ crystal versus CuI/AgI ratios.

(b) Core-Shell Type of $Cu_xAg_{1-x}I$ Crystal. In (a), (b) and (c) in Fig. 4, the X-ray diffraction curves of $Cu_xAg_{1-x}I$ crystal have doublet peaks of (111) and (222) planes, indicating solid CuI and solid-solution Cu_x-$Ag_{1-x}I$. Then, a mixed crystal may be considered to be either individual crystals or a core-shell type of crystal. In Fig. 5, we show the unit lattice constant in a solid solution for Ag/Cu ratios of 1/3, 1/1, and 3/1, respectively. For each Ag/Cu ratio the lattice constant was found to be considerably close to the constant of Ag I, 6.473 Å, in comparison with that predicted by the Vegard law. This Ag/Cu ratio dependency of the lattice constant may imply a core-shell model of the mixed crystal. Furthermore, in order to verify it, we

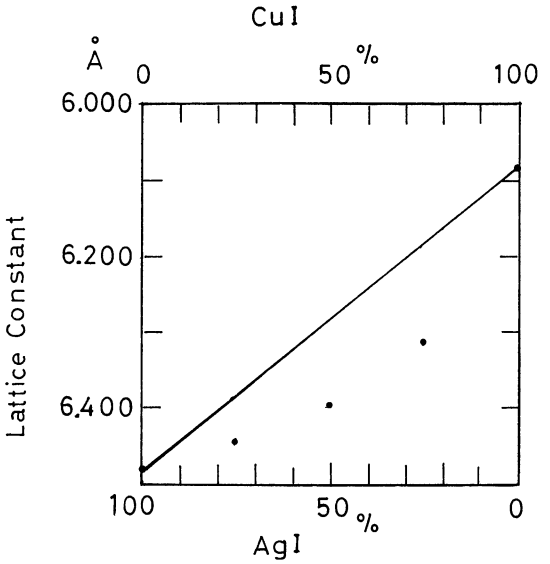

Fig. 5. The unit cell dimension of solid solution of core layer in the core-shell type of $Cu_xAg_{1-x}I$ crystal versus CuI/AgI ratios: The solid line is Vegard law.

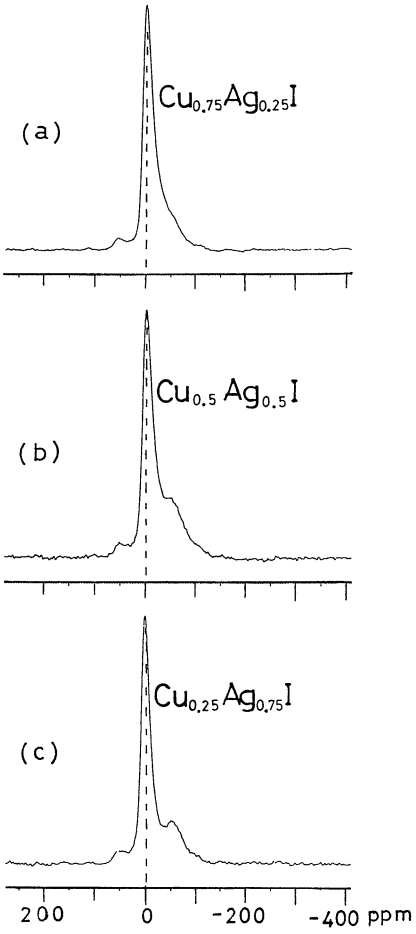

Fig. 6. ^{63}Cu MAS NMR spectra of core-shell types of $Cu_xAg_{1-x}I$ crystal versus CuI/AgI ratios.

have used the electron diffraction method(JEM 200CX). From a single crystal of about 0.1 μm size, we observed doublet diffraction spots. It will, thus, be proposed that a core-shell type of crystal consists of two layers: the inner(core) is CuI and outer(shell) a $Cu_xAg_{1-x}I$ solid solution, respectively.

For the MAS NMR spectra in (a)-(c) in Fig. 6, the signals did not shift and the line widths were much the same as those of the CuI. The signals have, however, a shoulder or lower peak in the higher-field side, as rations of AgI/CuI increase. Thus, the solid-solution $Cu_xAg_{1-x}I$ layer in this core-shell type of crystal may be thinner.

Discussion

A major finding of this work was to determine the local crystal structure of mixed crystals by the ^{63}Cu MAS NMR method and to link the structure analysis into the electronic structure of $Cu_xAg_{1-x}I$. In Table 1, the obtained chemical shifts and half line widths of tetrahedral -(CuI_4)- species in the solid-solution have different shifted values for three different AgI/CuI ratios. Concerning this, we have to give an interpretation from an analysis of the NMR chemical shifts.

Let's consider the local atomic structure of a unit lattice by replacing a Cu atom with Ag, in order to explain the chemical shift dependency of the ^{63}Cu spectral peak for different AgI/CuI ratios in the complete solid solution crystal. As shown in Fig. 7, we can suppose that five types of species, (-(Cu_4-I_4)-, -(Cu_3Ag-I_4)-, -(Cu_2Ag_2-I_4)-, -($CuAg_3$-I_4)- and -(Ag_4-I_4)-) exist in the unit lattice. In case (a), four T_d -CuI_4- species are seen to exist. For (b), three -CuI_4- species become C_{3v} symmetry by the movement of the location for the common I atom between three -CuI_4- and -AgI_4-, since a species of -AgI_4- exists. In (c) of Fig. 7 the existence of two species of -AgI_4- produces two C_{2v} species of -CuI_4-. In case (d), since there are three -AgI_4- species, a -CuI_4- species becomes another C_{3v} symmetry. For (e), four T_d -AgI_4- exist. We therefore believe that four kinds of symmetries of -CuI_4- may be observable as spectral intensities by ^{63}Cu MAS NMR.

In the case of a complete solid solution, $Cu_xAg_{1-x}I$, the existence of five species ((a) to (e) in Fig. 7) will follow the probability equation in proportion to the ratios of CuI/AgI. The probability for each case ((a)—(d)) corresponds to the NMR spectral intensity of four kinds of -CuI_4- symmetries. The equation is given by

$$P_{Cu_iAg_{4-i}I_4} = {}_4C_{4-i}X_{Cu}{}^iX_{Ag}{}^{4-i}, \quad (1)$$

where X_{Cu} and X_{Ag} denote the molar ratios of copper Cu and silver Ag, respectively. The subscript and superscript (i and $4-i$) correspond to the numbers of copper (Cu) and silver (Ag) and i ranges from 0 to 4: for example, we define Cu_0=Ag_0=1, $X_{Cu}{}^0X_{Ag}{}^4$=$X_{Ag}{}^4$ and so on. In Table 2, we show the calculated probability for the existence for the five species versus the ratio of CuI/AgI in a complete solid-solution crystal. Then, four symmetries of -CuI_4- in the table for the AgI/CuI ratios of 3/1, 1/1, and 1/3, respectively, can be considered to correspond to the NMR

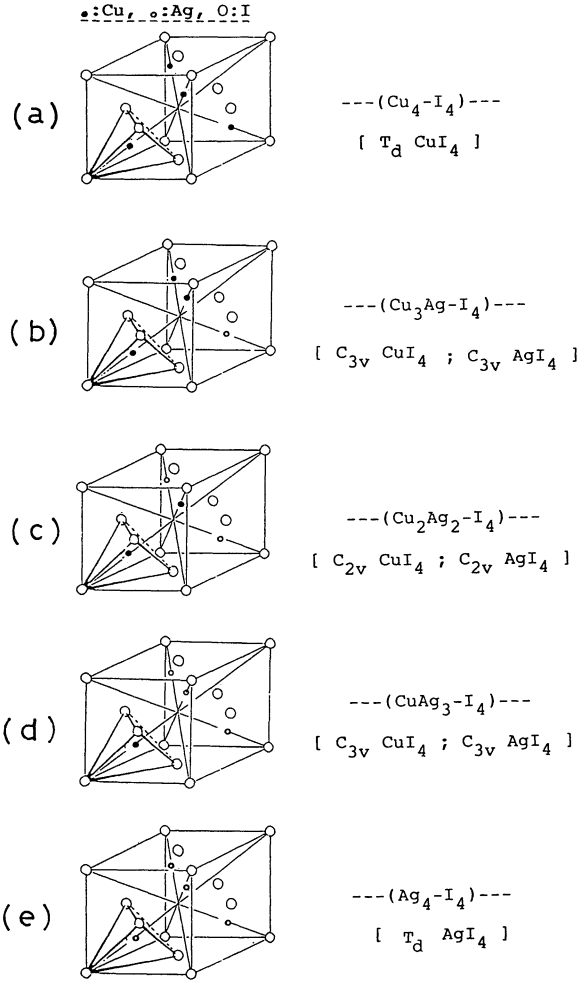

Fig. 7. The local atomic crystal structure of the unit lattice due to replacing Cu with Ag in the mixed $Cu_xAg_{1-x}I$ crystal.

Table 2. Existence Probability of Five Species for Complete Solid-Solution $Cu_xAg_{1-x}I$ Crystal in Propotion to Ratio of CuI/AgI

CuI/AgI ratio	-Cu_4I_4-	-Cu_3AgI_4-	-$Cu_2Ag_2I_4$-	-$CuAg_3I_4$-	-Ag_4I_4-
3/1	0.316	0.422	0.211	0.047	0.004
1/1	0.063	0.250	0.375	0.250	0.063
1/3	0.004	0.047	0.211	0.422	0.316

Table 3. Existence Probability of Five Species in the Shell for Core-Shell Types of Crystals Refered from X-ray Diffraction Profiles of (111) Plane in $Cu_xAg_{1-x}I$

AgI ratio	$-Cu_4I_4-$	$-Cu_3AgI_4-$	$-Cu_2Ag_2I_4-$	$-CuAg_3I_4-$	$-Ag_4I_4-$
0.56	0.04	0.19	0.36	0.31	0.10
0.71	0.01	0.07	0.25	0.42	0.25
0.86	0.00	0.01	0.09	0.35	0.55

spectral intensities in (a)—(c) of Fig. 3. Thus, the shift in Table 1 for each AgI/CuI ratio was considered to correspond to C_{3v} CuI_4 in a $-Cu_3AgI_4-$ cell, C_{2v} CuI_4 in a $-Cu_2Ag_2I_4-$ cell, and C_{3v} CuI_4 in a $-CuAg_3I_4-$ cell, respectively.

In this comple solid-solution, if there are four species of $-CuI_4-$ symmetries individually, we are supposed to observe four signals for such $-CuI_4-$ symmitry by this ^{63}Cu MAS NMR mathod: We were able to obtain three or four split signals for each AgI/CuI ratio by considering the half width, 256 Hz, for pure CuI. The results were, however, single component-like broader signals with high-field shifts. This indicates that there are four species of $-CuI_2-$ symmetries with slightly small deviations in the complete solid-solution. We can thus observe only a single component broader signal.

These differences between the $-CuI_4-$ symmetries affect the chemical shielding anisotropies, dipolar and quadrupolar coupling tensors of the Cu nucleus. In this crystal, we believe that the C_{2v} and C_{3v} $-CuI_4-$ species are nearly close to the T_d symmetry. Then, this Cu nucleus has smaller chemical shielding anisotropies and dipolar coupling constants. We calculated the chemical shift and half width of the dipolar contribution as less than a few ten ppm without MAS. The value will be averaged out to zero with MAS. Here, we can consider (second-order quadrupolar interaction)$\gg$(second order chemical shielding anisotropies), (second-order dipolar interaction). We, thus, assume that the obtained shift (14—33 ppm) and half width differences (1400—1800 Hz) are due to a second-order quadrupolar interaction. An estimation of the quadrupolar coupling constants was made from the obtained shifts.[5]

For the ^{63}Cu MAS NMR spectrum the central transition (I=3/2, M=1/2), the second-order quadrupolar shift of center of qravity is given as

$$\sigma_{qs}(I = 3/2, m=1/2) = -(C_q^2/40\nu_L^2)(1 + \eta^2/3), \quad (2)$$

where the quadrupole coupling constant(C_q) and the Larmor frequency(ν_L) are both given either in Hz. In the case of the shifts given in Table 1, we obtained $C_q \simeq 0.27$, 0.37, and 0.41 MHz for $\eta=0$ and $\nu_L=71.47$ MHz. In Table 1, we show the quadrupole coupling constants and the CuI_4 symmetry which corresponds to the shifts. The e^2qQ values appear to reflect the field gradient around a copper(I) nucleus in a mixed crystal: it depends on the densities of the 3d and 4p electrons of the Cu atom.[8]

For a core-shell type $Cu_xAg_{1-x}I$ crystal, the core consists of the $-(Cu_4-I_4)-$ species in the unit lattice. On the other hand, by using Eq. 1 and the Vegard law in Fig. 5 from the X-ray diffraction curves, the shells are found to be made up of each component of five species for the CuI/AgI ratios in Table 3. This result indicates a shoulder or lower peak of the ^{63}Cu MAS NMR spectra in the high- field side of Fig. 6. For an AgI/CuI ratio of 1/1, a shift of 41 ppm was estimated as 0.46 MHz of e^2qQ. In the case of a 3/1 ratio, a shift of 52 ppm was evaluated as being 0.51 MHz of e^2qQ. This implies that the deviation of the symmetries in the shell is larger than in a complete solid solution.

References

1) T. H. James, "The Theory of the Photographic Process," 4th ed, Macmillan, New York (1977).

2) a) C. S. Yannoni, *Acc. Chem. Res.*, **15**, 201 (1982). b) J. R. Lyerla, C. S. Jannoni, and C. A. Fyfe, *ibid.*, **15**, 208 (1982).

3) G. E. Maciedl, *Science*, **226**, 282 (1984).

4) D. Muller, W. Gessner, H.-J. Behrens, and G. Scheler, *Chem. Phys. Lett.*, **79**, 59 (1981).

5) D. Kundla, A. Samoson, and E. Lippma, *Chem. Phys. Lett.*, **83**, 229 (1981).

6) D. Freude and H.-J. Behrens, *Cryst. Res. Technol.*, **16**, 36 (1981).

7) L. Vegard and G. Skofteland, *Arch. Math. Naturv.*, **45**, 163 (1942).

8) K. Endo, K. Yamamoto, K. Deguchi, and K. Matsushita, *Bull. Chem. Soc. Jpn.*, **60**, 2803 (1987).